EFFECT OF FLOW DISTRIBUTION IN PARALLEL HEAT EXCHANGER NETWORKS: USE OF THERMO-HYDRAULIC CHANNELING MODEL IN REFINERY OPERATION

E. M. Ishiyama[1*] and S. J. Pugh[1]

[1] Heat Transfer Research, Inc. P.O. Box 1390, Navasota, TX 77868 USA
*Corresponding author: edward.ishiyama@htri.net

ABSTRACT

Parallel branches are commonly observed in industrial heat exchanger networks. Despite the important relationship between flow distribution and network efficiency, not all parallel branches comprise of flow controllers or not least, flow measurements. When the network is subject to fouling, uncontrolled flow branches can introduce undesired phenomenon such as thermo-hydraulic channeling (THC) [presented at the 2007 HEFC conference; Ishiyama et al., Effect of fouling on heat transfer, pressure drop and throughput in refinery preheat trains]. Recent analysis of crude preheat train heat exchangers has shown the need to use THC models, in particular, for situations where there is insufficient flow measurement data, especially in non-symmetric branches. This paper revisits the THC model and highlight practical importance of the THC phenomenon through analysis of plant data. The hydraulic aspect of the analysis is strongly linked to the knowledge of deposit thermal conductivity. A case study of a section of a crude refinery heat exchanger network is used to illustrate the use of thermo-hydraulic models in data reconciliation to understand flow imbalances caused due to differences in operating conditions and fouling of heat exchangers in each branch of a parallel network.

INTRODUCTION

Heat exchanger networks (HENs) are an integral part of many industrial operations. It is common for HENs to consist of exchangers in parallel branches that are usually non-symmetric. Such arrangements can be a result of network design to maximize heat recovery or effort to reduce pressure drop while facilitating cleaning of the exchangers. Control of stream flows in branches requires a good understanding of the performance of individual exchangers as well as their interaction within the network. However, despite the importance of flow control, some parallel branches in HENs have streams not only without flow control but also without flow measurements.

Parallel branches can consist of different exchanger geometry or other differences (e.g., different degree of cleaning) and flow imbalances could spontaneously occur in the absence of flow controllers. Such situations were discussed by Ishiyama et al. (2007) and a phenomena called 'thermo-hydraulic channeling (THC)' was introduced (Ishiyama et al., 2008). In the absence of flow controllers, the pressure drop across branches is the same and therefore the flow will divert to maintain the common pressure drop if flow resistances change in the branches. Fouling is a common cause to change flow resistance during operation. If fouling in the exchangers is a function of surface shear and/or temperature, the net result is that the fouling rate in the branches will change and continue to divert flow in the branches to maintain the common pressure drop. This positive feedback phenomenon is termed THC. In Ishiyama et al. (2008), deposit thermal conductivity was highlighted as a key parameter in determining the thermo-hydraulic behavior.

Occurrence of THC highlights possibility of a substantially impaired network performance and flow control and optimization strategies are recognized to be important (e.g., Borges et al. (2009), de Oliveira Filho et al. (2009) and Assis et al. (2013, 2015)). Da Silva et al. (2015) discussed the use of nonlinear programming problem formulation to solve flow split optimization to minimize both heat and production losses for networks subject to fouling and THC.

Thermal and hydraulic analysis and role of deposit thermal conductivity remains a topic of interest among researchers; recent publication by Diaz-Bejarano et al. (2017) uses a distributed model to emphasize the relationship.

Fouling of micro channels are also a key area where thermo-hydraulic aspects are important. Due to the high surface to area ratio, handling the fouling/blockage of fouled channels are different compared to macro devices (Schoenitz et al., 2015).

This manuscript aims to discuss the use of thermo-hydraulic models to assist data reconciliation analysis for crude refinery HENs with parallel branches, in the absence of flow controllers or individual flow measurements. In such situations flow across branches will spontaneously adjust to

ISBN: 978-0-9984188-0-3; Published online www.heatexchanger-fouling.com

achieve the common pressure drop. This could be used to calculate the amount of flow across each branch.

The value of deposit thermal conductivity also affects the analysis. Extraction of deposit thermal conductivity from plant measurements are presented separately at this conference (Ishiyama et al., 2017).

MODEL FORMULATION

For illustration, model formulation discussed here is for a heat exchanger network consisting of parallel branches with each branch consisting of shell-and-tube heat exchangers in series (Fig 1).

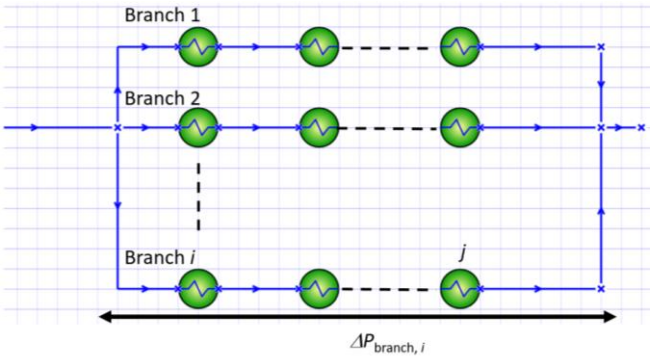

Fig 1 Schematic layout of a heat exchanger network consisting of parallel branches. The circles indicate shell-and-tube heat exchangers. The streams shown are connected to the tube side of the exchangers. The shell-side streams are not shown in this figure.

Network hydraulic simulation

For a heat exchanger network consisting of n parallel branches, let $\Delta P_{branch,i}$ the pressure drop across a branch, i:

$$\Delta P_{branch,i} = \sum_{j=1}^{n} \Delta P_{j,i} + \Delta P_{piping,i} \quad (1)$$

Here, $\Delta P_{j,i}$ is the pressure drop of exchanger j at branch i and $\Delta P_{piping,i}$ is the sum of pressure drop across piping and fittings of branch i.

If the flow associated with the branch is connected to the tube side of the exchanger, $\Delta P_{j,i}$ is calculated as the sum of the nozzle loss, tube pressure drop, tube entrance, expansion and turn around losses. A simplified representation takes the form:

$$\Delta P_{j,i} \approx a\, m_i{}^2 + b\, m_i{}^{(1.75\sim 2)} (d_i - 2\delta)^{-(4.75\sim 5)} \quad (2)$$

where δ is the deposit thickness, d_i is the tube internal diameter, m_i is the mass flow rate across branch i; a and b are dimensional constants.

If the flow associated with the branch is connected to the shell side of the exchanger, then the shell-side pressure drop is calculated using a stream analysis methodology.

For simplicity, in this manuscript, the $\Delta P_{piping,i}$ is ignored (i.e., it is assumed that $\sum_{j=1}^{n} \Delta P_{j,i} \gg \Delta P_{piping,i}$). Incorporating pressure drops across piping and fittings in network simulations are discussed elsewhere (Ishiyama et al. (2009)).

In the absence of flow control, the flow across the branches ($m_{1,2,..,i}$), would spontaneously adjust to give equal pressure drop across the branch:

$$\Delta P_{branch,1} = \Delta P_{branch,2} = \cdots = \Delta P_{branch,i} \quad (3)$$

Heat transfer

The overall heat transfer coefficient, U, of an exchanger is evaluated based on the sum of resistances in series:

$$\frac{1}{U} = \frac{1}{h_o} + R_{f,o} + \frac{d_o ln\left(\frac{d_o}{d_i}\right)}{2\lambda_w} + \frac{d_o}{d_i} R_{f,i} + \frac{d_o}{d_i}\frac{1}{h_i} \quad (4)$$

Here h_i is the internal heat transfer coefficient, h_o the external heat transfer coefficient, $R_{f,o}$ the external fouling resistance, $R_{f,i}$ the internal fouling resistance, δ the deposit thickness and d_i and d_o are the internal and external tube diameters, respectively. $R_{f,o}$ is taken to be zero for exchangers with product on the shell side and in the absence of product stream fouling, making $R_{f,i}$ equal to the overall thermal resistance of the deposit, R_f.

Both h_i and h_o are calculated via semi-empirical relationships. Calculation of h_o is based on a stream analysis methodology.

The thickness of the deposit layer, δ, is estimated by assuming a deposit thermal conductivity, λ_f, and using the thin slab approximation:

$$\delta = \lambda_f R_f \quad (5)$$

δ is used to simultaneously solve the exchanger pressure drop (Equation (2)).

The thermal performance of the exchanger can also be expressed as a fouling Biot number, Bi_f, given by:

$$Bi_f = U_{cl} R_f \quad (6)$$

where U_{cl} is the overall fouling resistance in the clean condition.

It is common for refineries to have shells in series without temperature measurements between shells. In such instances, additional constraints would be required to solve for fouling resistances among shells. One such approach proposed by Ishiyama et al. (2011) was to determine the ratios of fouling resistances as the ratios of the fouling rates of each shells at its clean condition.

$$R_{f,1} : R_{f,2} : \cdots : R_{f,j} = \dot{R}_{f,1,cl} : \dot{R}_{f,2,cl} : \cdots : \dot{R}_{f,j,cl} \quad (7)$$

Here, $R_{f,j}$ is the fouling resistance and $\dot{R}_{f,j,cl}$ is the fouling rate at clean condition for exchanger j, respectively. In this manuscript, $\dot{R}_{f,j,cl}$, is formulated as a function of shear stress

only as the exchanger group in interest is located at the colder section of the heat exchanger network and presented by:

$$\dot{R}_{f,j,cl} = f(\tau_{j,cl}) \quad (8)$$

Here $\tau_{j,cl}$ is the shear stress of exchanger j at clean condition. The analysis was performed using a commercial software tool (HTRI SmartPM).

CASE STUDY

The case study illustrated here is based on a section of a crude preheat train in a US refinery. The section (in Fig 2) is situated immediately before the desalter. Other heat exchanger networks connected upstream and downstream of this section are not discussed here. The un-desalted crude entering the heat exchanger network is divided to three parallel branches and passes through the tube side of the exchangers E1A/E1B, E2A/E2B and E3A/E3B, respectively. The product stream passes through the shell side of the exchangers. Details of the exchangers are summarized in Table 1. The units E1A and E1B have different areas and are also different from the rest of the shells (E2A/B and E3A/B). Even though E2A/B and E3A/B have the same surface area, the reported tube-side velocities are different as the tube-side passes are different. i.e., the three branches have different flow resistances due to the design. For the same mass flow rate in each branch (65 kg s^{-1}), branch 3 has the highest calculated pressure drop (1.78 bar, i.e., highest flow resistance) and branch 2 has the lowest pressure drop (0.28 bar, i.e., lowest flow resistance).

Shell E3B has the highest overall heat transfer coefficient and the highest heat duty (at the conditions summarized below Table 1). The crude side Prandtl number of E1A, E2A and E3A are larger than those of E1B, E2B and E3B, respectively, due to the higher crude viscosity.

The temperatures of the crude stream and the product stream entering the section are measured and labelled as $T_{c,in}$ and $T_{h,in}$ in Fig 1, respectively. The total volumetric flow of the streams entering the section is also measured elsewhere in the network. As the volumetric flow is known, the calculated total mass flow rates of the crude and the product stream in Fig 1 are labelled as $m_{c,total}$ and $m_{h,total}$, respectively. The individual branch flow rates are unmeasured for both the crude and the product streams.

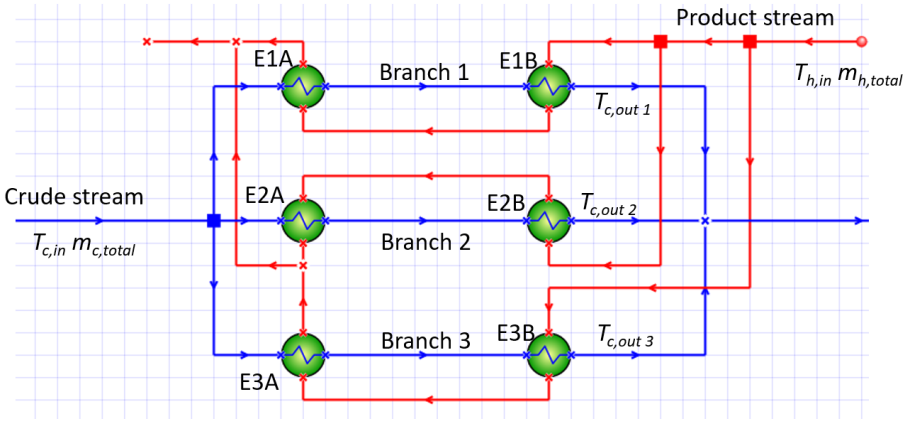

Fig 2 Schematic layout of a section of the preheat train. The circles indicate shell-and-tube heat exchangers.

Table 1: Summary of exchanger areas and operations in Fig 2.

Shell	Area (m^2)	*Tubeside velocity (m s^{-1})	*Clean tubeside pressure drop (bar)	*Clean overall heat transfer coefficient (W m^{-2} K^{-1})	*Heat duty (MW)	Crude-side Prandtl number
E1A	210	2.3	1.52	280	1.89	160
E1B	230	1.1	0.17	270	1.88	73
E2A	265	0.9	0.13	180	1.58	170
E2B	265	1.0	0.15	190	1.46	90
E3A	265	1.9	0.96	210	1.59	170
E3B	265	1.9	0.82	430	2.44	74

*For an assumed crude inlet temperature and flow of 105 °C and 65 kg s^{-1} for each branch; product stream inlet temperature and flow of 215 °C and 35 kg s^{-1}.

ISBN: 978-0-9984188-0-3; Published online www.heatexchanger-fouling.com

The temperature of the product stream outlet is also unmeasured. So the actual heat duty of the network is unknown. However, the refinery had previously assumed equal mass flow rates across each branch for both the crude and the product streams. This is incorrect as the flow across the branch would spontaneously adjust to achieve a common pressure drop. The measured flows and temperatures are reported in Fig 3.

For the purposes of illustration, a short operating period of eleven weeks was selected. The recorded crude stream outlet temperatures are different for $T_{c,out\ 1}$, $T_{c,out\ 2}$ and $T_{c,out\ 3}$ as the mass flow across the branches as well as the geometries of the units are different.

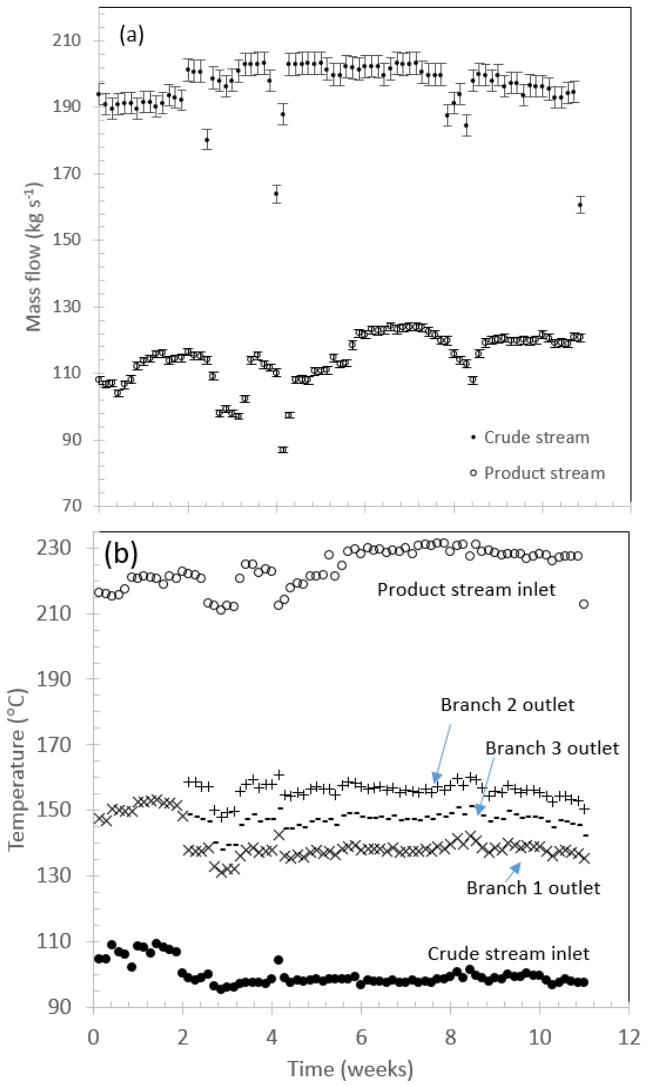

Fig 3 (a) Total mass flow rate and (b) temperature measurements collected for the network presented in Fig 2. The filled and hollow circle present crude stream inlet and product stream inlet conditions respectively. The cross, dash and plus show crude stream outlet temperatures of each branch. The error bars on (a) is based on a 1% error on volumetric flow measurement and an error in crude °API of ±1. The error in product stream density was assumed to be negligible. The error in the temperature measurements are ±1 °C and not presented in the graph.

The methodology described through equations (1) to (6) were used to calculate the flow across the branches 1 to 3. The product stream was assumed to be non-fouling, hence fouling was only assumed to occur on the tube side. Deposit thermal conductivity dictates the thickness and flow constriction based on equations (2) and (5). As the calculation is sensitive to the deposit thermal conductivity, two values of thermal conductivities (0.1 and 0.2 W m^{-1} K^{-1}) were assumed to illustrate the influence on the calculation. The assumption of deposit thermal conductivity was required due to the absence of the total network duty.

The calculated mass flow rates and the flow fractions of each branch are summarized in Fig 3. Fig 3 (a), (b) and (c); (d), (e) and (f) share a common time axis. The flow fraction of a branch *i* is calculated via:

$$F_i = \frac{m_i}{m_{total}} \tag{9}$$

Here m_i is the mass flow across branch *i*, and m_{total} the sum of mass flow across all branches.

The mass flow rates among branches are significantly different compared to having an equal flow across the three branches (which would give ~65 kg s^{-1} per branch). Hollow circles and crosses represent results based on deposit thermal conductivities of 0.1 and 0.2 W m^{-1} K^{-1}, respectively.

As branch 3 has the highest flow resistance (from Table 1), the stream has the lowest mass flow rate. The highest mass flow is on branch 2 which comprises of the lowest resistance.

The flow across branch 1 is closer to branch 3 compared to branch 2 as the flow resistances in branches 1 and 3 are similar when the shells are clean. When the deposit thermal conductivity is increased, the flow deviation across the three branches increases. This is due to the higher deposit thickness calculated from Equation (5), which results in a higher flow resistance. Hence the flow across branch 3 is further decreased for λ_f of 0.2 W m^{-1} K^{-1} compared to 0.1 W m^{-1} K^{-1}. If the operation continue, this shows that flow fraction of branch 3 (Fig 4 (f)) gradually diminishes with fouling. Due to the different flow fields (and hence the temperature field), the thermo-hydraulics of each individual shells would differ.

The thermo-hydraulic performance of each shell in Fig 2 is summarized in Fig 5. Fig 5 (a), (b), (c), (d), (e), and (f) share a common abscissa and an ordinate to allow direct comparison of performances among shells. Each plot shows the change in Bi_f over $\Delta P_{i,j}/\ \Delta P_{i,j,cl}$. The time scale is secondary and the plot is for the operating period where the monitoring data were collected (~ 11 week period). As a reference, when Bi_f reaches 1, the duty heat transfer coefficient has reached half of its clean value. When $\Delta P_{i,j}/\ \Delta P_{i,j,cl}$ reaches 2, the flow resistance has doubled compared to the clean state for the specific flow rate.

Equal flow across branches (Fig 5, hollow triangles):

The hollow circles represent the performances of each shells when equal flow across the three branches are assumed. This was the original assumption of the plant. As an illustration, a deposit thermal conductivity of 0.1 W m^{-1} K^{-1} was assumed. The thermal and hydraulic impact of fouling on shells E1A is negligible (Fig 5 (a)).

ISBN: 978-0-9984188-0-3; Published online www.heatexchanger-fouling.com

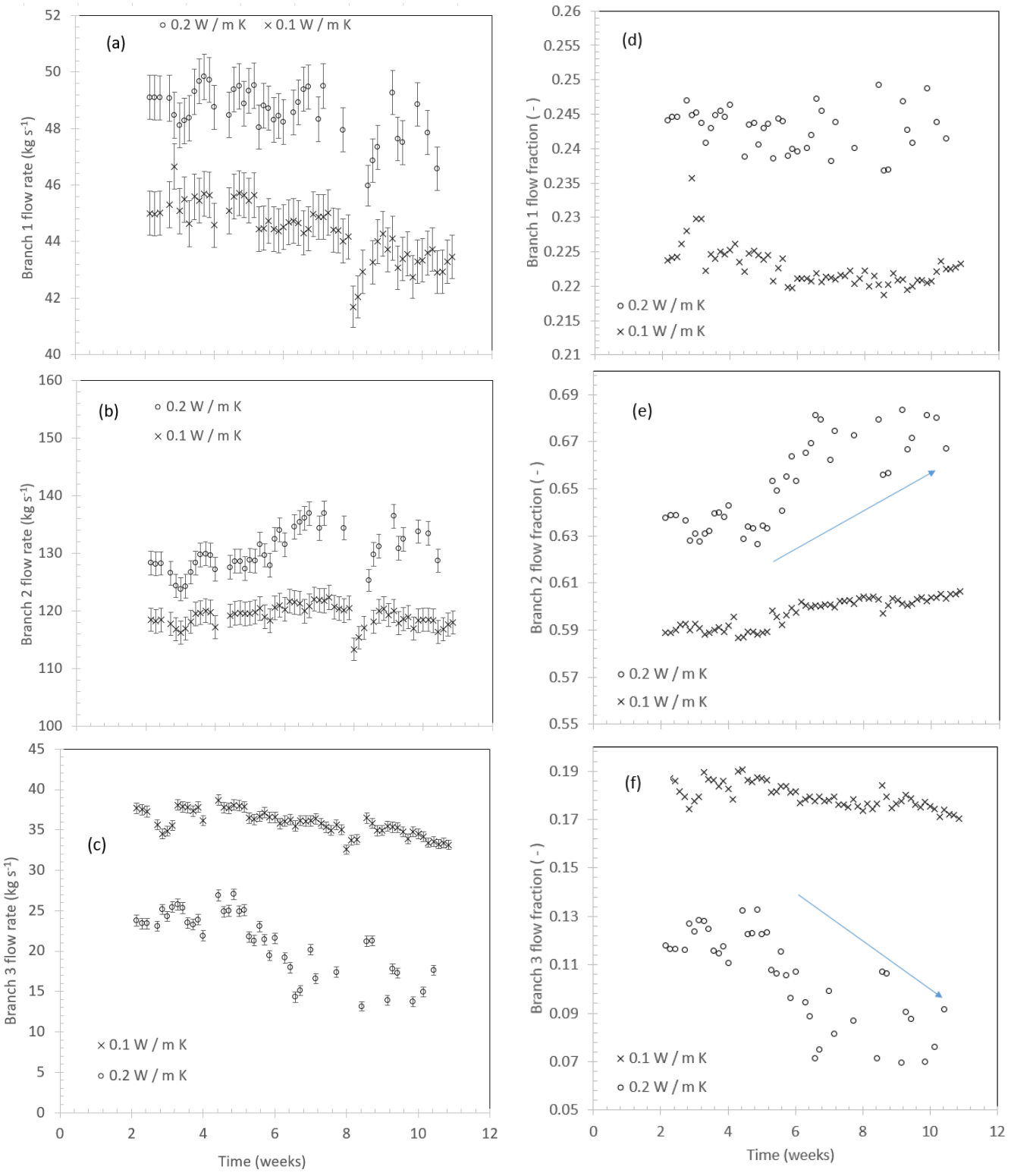

Fig 4 Mass flow rate and flow fraction assuming equal pressure drop across branches 1 to 3. Figures (a), (d) represent branch 1; figures (b), (e) represent branch 2 and figures (c), (f) represent branch 3, respectively. The cross and hollow circle are results based on assuming deposit thermal conductivity values of 0.1 and 0.2 W m^{-1} K^{-1}, respectively. The arrows in figures (f) and (g) represents trend to flow fraction variation. The error bars in (a), (b) and (c) represent the maximum and minimum flows calculated based on the mass flow errors in Fig 3.

ISBN: 978-0-9984188-0-3; Published online www.heatexchanger-fouling.com

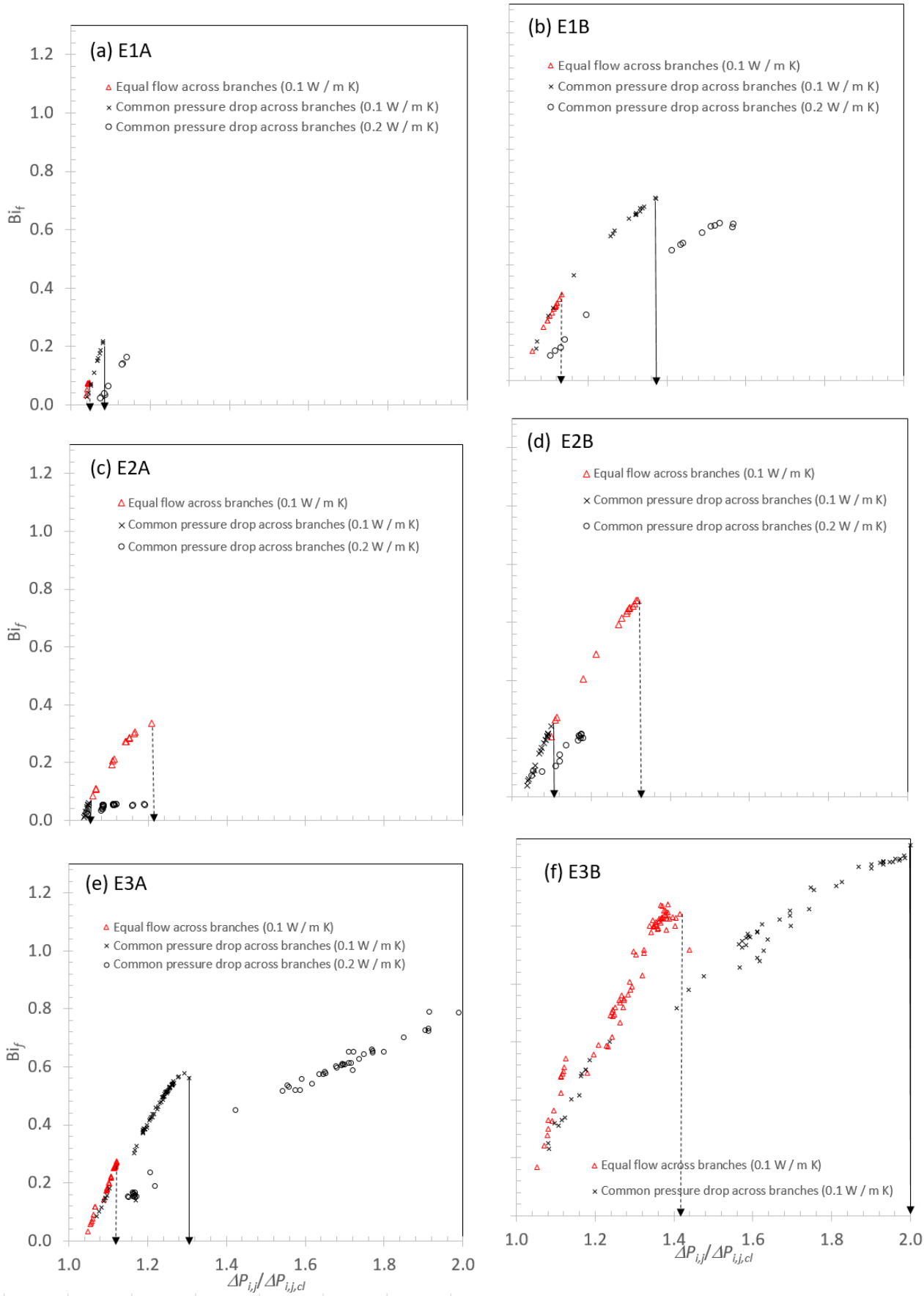

Fig 5 Fouling Biot number against the $\Delta P_{i,j}/\Delta P_{i,j,cl}$. Labels (a), (b), (c), (d), (e) and (f), represent shells E1A, E1B, E2A, E2B, E3A and E3B, respectively. The hollow triangles represent result assuming equal mass flow across branches 1 to 3 with λ_f of

ISBN: 978-0-9984188-0-3; Published online www.heatexchanger-fouling.com

0.1. The crosses and hollow circles represent result assuming equal pressure drop across branches and λ_f of 0.1 and 0.2 W m^{-1} K^{-1}, respectively. The hollow circles are not shown in (f) as the $\Delta P_{i,j}/\Delta P_{i,j,cl}$ is outside the scale (i.e., above 2.0). The dashed and the solid vertical guide lines indicate the increase in hydraulic resistance after 11-week period.

Units E1B, E2A and E3A all suffer minor reduction in thermal performance but up to ~10 – 20 % increase in flow resistance (Fig 5 (b), (c) and (e)).

E2B and E3B appears to suffer the most with its thermal performance reaching half of the original clean state and flow resistance increasing by up to 40%. These shells appears to be a bottleneck in terms of maintaining flow in both branches 2 and 3. Under the absence of flow controllers it is not possible to achieve equal flows across the branches as the sum of the pressure drop of shells in each branch are different (from Table 1).

Equal pressure drop across branches (Fig 5, cross and hollow circles):

The cross and triangle represent performances of each shell when equal pressure drop across the branches are assumed. The cross and the triangle are based on deposit thermal conductivity values of 0.1 W m^{-1} K^{-1} and 0.2 W m^{-1} K^{-1}, respectively. For both λ_f of 0.1 and 0.2 W m^{-1} K^{-1} the flow fraction in branch 3 gradually reduces, due to the shells E3A and E3B reaching their hydraulic limits. The reduction is larger for the case when λ_f is 0.2 W m^{-1} K^{-1}. The data for E3B when λ_f is 0.2 W m^{-1} K^{-1} is not plotted on the graph as most of the data were outside the common scale of Fig 5.The flow fraction across branch 1 remains almost constant while the fraction in branch 2 gradually increases. This illustrates the positive feedback effect that would be observed when thermo-hydraulic channeling occur.

Impact on cleaning schedule

When equal flow across branches are assumed the thermal penalty of fouling on E2B is significantly high compared to E1B (see Fig 5(b) and (d)). However, the opposite is evident when comparing in the equal pressure drop assumption. When the plant is not throughput limited, then the decision on which shell to clean would be completely different, for this illustration, based on whether the calculation is done for equal throughput or equal pressure drop scenarios.

Comparison of network operation with equal mass flow across branches to equal pressure drop between branches:

Comparing the hollow triangles (equal mass flow across branches) with the crosses, and the hollow circles (equal pressure drop across branches), it is noticeable that the equal flow calculation under predicts the fouling penalties in exchangers E1A, E1B, E3A and E3B and over predict the fouling penalties for exchangers E2A and E2B (see the dashed and solid vertical lines in Fig 5, which shows the increase in hydraulic penalty after 11 weeks of operation).

From the assumption of equal flow across the branches, it is likely that branch 2 will reach a defined thermal or hydraulic limit during the cause of the network operation. However, this is false in the presence of THC. The units E3A and E3B hydraulically limits the performance of branch 3, which explains the flow divergence to branches 1 and 3 with THC. Incorrectly identifying the branch that debottleneck the network performance will result in cleaning of incorrect units when optimal cleanin schedules are formulated.

As the calculated flows assuming equal pressure drop across the branches were significantly different from the assumption of equal flow across branches, the resulting network duty would be different. The difference in the calculated network heat duties were represented as a percentage, ψ, given by:

$$\varphi = \frac{Q_m - Q_{\Delta P}}{Q_{\Delta P}} \times 100\% \quad (10)$$

Here, Q_m is the network duty assuming equal mass flow rate across branches and $Q_{\Delta P}$ is the network duty assuming equal pressure drop across branches. Network duty is calculated as the sum of the heat duties of the individual shells.

For the cases described in Fig 4, φ was calculated for deposit thermal conductivities of 0.1 and 0.2 W m^{-1} K^{-1}, respectively. The difference in heat duties are significant and have reached upto ~ 10% for the case where λ_f of 0.2 W m^{-1} K^{-1} was assumed.

Throughout the manuscript, the deposit thermal conductivity was assumed to remain unchanged and the surface roughness to remain to that of the clean tube. However, deposit ageing (e.g., Ishiyama et al. (2010), Wilson et al. (2009)) and surface roughness (e.g., Coletti et al. (2010), Ishiyama et al. (2017)) would have an impact on the thermo-hydraulics.

If either the total crude stream outlet temperature or the total product stream outlet temperature is measured, then it would eliminate the uncertainty in obtaining the network duty. That is, when the total network duty is known (through the additonal temperature measurement), it would be possible to computationally identify the combination of mass flow fraction and the deposit thermal conductivity which would result in the specified network duty while satisfying the condition for equal pressure drop between branches.

CONCLUSIONS

1. Monitoring data were collected from an industrial heat exchanger network with three parallel branches which operate in the absence of flow controllers or individual flow measurements for each branch. Historical flows across each branch were estimated by calculating the network thermo-hydraulics such that pressure drop was equal in each branch.

2. The calculated mass flow across each branch revealed significant difference compared to assuming equal flow across branches. Flow diversion was observed to occur across the branches with time.

3. The plant previously evaluated network performance assuming equal flow across the branches. This was compared with the results obtained from the method in the manuscript, which revealed a difference of up to ~ 10% in the calculated heat duty.

ISBN: 978-0-9984188-0-3; Published online www.heatexchanger-fouling.com

4. The calculated thermal and hydraulic performance of each shell showed that when assuming equal flow, the exchangers in branch 2 reaches the thermal limit much earlier than in branch 1. However, the result is opposite when assuming equal pressure drop across branches. This has affected future operating decision such as cleaning scheduling.

NOMENCLATURE

a	dimensional constant, kg m^{-3} s^{-2}
b	dimensional constant, $m^{4.75 \sim 5}$ $s^{-(1.75 \sim 2)}$
Bi_f	fouling Biot number
d_i	internal tube diameter, m
d_o	external tube diameter, m
h_i	internal film transfer coefficient, W m^{-2} K^{-1}
h_o	external film transfer coefficient, W m^{-2} K^{-1}
m	mass flow rate, kg s^{-1}
Q_m	network duty assuming equal mass flow rate across parallel branches, MW
$Q_{\Delta P}$	network duty assuming equal mass flow rate across parallel branches, MW
R_f	fouling resistance, m^2 K W^{-1}
$\dot{R}_f$	rate of change in overall fouling resistance, m^2 K J^{-1}
t	time, days
T	temperature, K
U	overall heat transfer coefficient, W m^{-2} K^{-1}

Greek

δ	deposit thickness, m
ΔP	pressure drop, Pa
φ	percentage difference in calculated network duty, -
λ	thermal conductivity, W m^{-1} K^{-1}
τ	shear stress, Pa

Subscript

branch	across a network branch
c	cold stream
cl	clean
f	foulant layer
h	hot stream
i	i^{th} heat exchanger
in	inlet
j	j^{th} branch
out i	outlet *i* (*i* = 1, 2 or 3).
n	total number of heat exchanger in a branch
piping	across piping and fittings
total	total flow
w	wall

RERERENCES

Assis, B. C. G., Gonçalves, C. de O., Liporace, F. S., Oliveira, S. G., Queiroz, E. M., Pessoa, F. L. P., and Costa, A. L. H. (2013). Constrained thermohydraulic optimization of the flow rate distribution in crude preheat trains. *Chem. Eng. Res. Des.* 91, 1517–1526.

Assis, B. C. G., Lemos, J. C., Liporace, F. S., Oliveira, S. G., Queiroz, E. M., Pessoa, F. L. P., and Costa, A. L. H. (2015). Dynamic optimization of the flow rate distribution in heat exchanger networks for fouling mitigation. *Ind. Eng. Chem. Res.* 54, 6497–6507.

Borges, J. L., Queiroz, E. M., Pessoa, F. L. P., Liporace, F. S., Oliveira, S. G., and Costa, A. L. H. (2009). Fouling management in crude oil preheat trains through stream split optimization. *Computer Aided Chemical Engineering*. 27, 1587-1592.

Coletti, F., Ishiyama, E. M., Paterson, W. R., Wilson, D. I., and Macchietto, S. (2010). Impact of deposit aging and surface roughness on thermal fouling: Distributed model. *AIChE J.* 56, 3257–3273.

Da Silva, R. L., Costa, A. L. H., and Queiroz, E. M. (2015). Stream flow rate optimization for fouling mitigation in the presence of thermohydraulic channelling. In *Heat Exchanger Fouling and Cleaning*, (Dublin, Ireland).

Diaz-Bejarano, E., Coletti, F., and Macchietto, S. (2017). Thermo-hydraulic analysis of refinery heat exchangers undergoing fouling. *AIChE J.* 63, 984–1001.

Ishiyama, E. M., Paterson, W. R., and Wilson, D. I. (2007). The effect of fouling on heat transfer, pressure drop and throughput in refinery preheat trains: Optimisation of cleaning schedules. In *7th International Conference on Heat Exchanger Fouling and Cleaning - Challenges and Opportunities* (Tomar, Portugal).

Ishiyama, E. M., Paterson, W. R., and Wilson, D .I. (2008). Thermo-hydraulic channelling in parallel heat exchangers subject to fouling. *Chem. Eng. Sci.* 63, 3400–3410.

Ishiyama, E. M., Paterson, W. R., and Wilson, D. I. (2009). Platform for techno-economic analysis of fouling mitigation options in refinery preheat trains. *Energy Fuels* 23, 1323–1337.

Ishiyama, E. M., Coletti, F., Macchietto, S., Paterson, W. R., and Wilson, D. I. (2010). Impact of deposit ageing on thermal fouling: Lumped parameter model. *AIChE J.* 56, 531–545.

Ishiyama, E. M., Pugh, S. J., Wilson, D. I., Paterson, W. R., and Polley, G. T. (2011). Importance of data reconciliation on improving performances of crude refinery preheat trains. In *AIChE Annual Meeting, Conference Proceedings* (Chicago: AIChE).

Ishiyama, E. M., Falkeman, E .S., Wilson, D. I., and Pugh, S. J. (2017). Quantifying implications of deposit ageing from crude refinery preheat train data. In *Heat Exchanger Fouling and Cleaning* (Madrid, Spain).

de Oliveira Filho, L. O., Liporace, F. S., Queiroz, E. M., and Costa, A. L. H. (2009). Investigation of an alternative operating procedure for fouling management in refinery crude preheat trains. *Appl. Therm. Eng.* 29, 3073–3080.

Schoenitz, M., Augustin, W., and Scholl, S. (2015). Challenges in cleaning microstructured devices. *Food Bioprod. Process.* 93, 283–288.

Wilson, D. I., Ishiyama, E. M., Paterson, W. R., and Watkinson, A. P. (2009). Ageing: Looking back and looking forward. (Schladming, Austria), pp. 221–230.